Published in final edited form as:
J Nutr Biochem. 2013 December ; 24(12): 2168–2174. doi:10.1016/j.jnutbio.2013.08.009.

Resveratrol protects against polychlorinated biphenyl-mediated impairment of glucose homeostasis in adipocytes

Nicki A. Baker[1], **Victoria English**[2], **Manjula Sunkara**[3], **Andrew J. Morris**[3], **Kevin J. Pearson**[1], and **Lisa A. Cassis**[1,2,*]

[1] Graduate Center for Nutritional Sciences, University of Kentucky, Lexington, Kentucky, 40536-0200

[2] Department of Molecular and Biomedical Pharmacology, University of Kentucky, Lexington, Kentucky, 40536-0200

[3] Division of Cardiovascular Medicine, University of Kentucky, Lexington, Kentucky, 40536-0200

Abstract

Resveratrol (RSV) is a plant polyphenol that exhibits several favorable effects on glucose homeostasis in adipocytes. Recent studies from our laboratory demonstrated that coplanar polychlorinated biphenyls (PCBs) that are ligands of the aryl hydrocarbon receptor (AhR) impair glucose homeostasis in mice. PCB-induced impairment of glucose homeostasis was associated with augmented expression of inflammatory cytokines in adipose tissue, a site for accumulation of lipophilic PCBs. This study determined if RSV protects against PCB-77 induced impairment of glucose disposal *in vitro* and *in vivo*, and if these beneficial effects are associated with enhanced nuclear factor erythoid 2-related factor 2 (Nrf2) signaling in adipose tissue. PCB-77 increased oxidative stress and abolished insulin stimulated 2-deoxy-D-glucose (2DG) uptake in 3T3-L1 adipocytes. These effects were restored by RSV, which resulted in a concentration-dependent increase in NAD(P)H:quinone oxidoreductase 1 (NQO1), the downstream target of Nrf2 signaling. We quantified glucose and insulin tolerance and components of Nrf2 and insulin signaling cascades in adipose tissue of male C57BL/6 mice administered vehicle or PCB-77 (50 mg/kg) and fed a diet with or without resVida® (0.1%, or 160 mg/kg/day). PCB-77 impaired glucose and insulin tolerance, and these effects were reversed by RSV. PCB-77 induced reductions in insulin signaling in adipose tissue were also abolished by RSV, which increased NQO1 expression. These results demonstrate that coplanar PCB-induced impairment of glucose homeostasis in mice can be prevented by RSV, potentially through stimulation of Nrf2 signaling and enhanced insulin stimulated glucose disposal in adipose tissue.

* To Whom Correspondence should be addressed: Telephone: 859-323-4933, ext. 81400; Fax: 859-257-3646; lcassis@uky.edu.

Keywords

Resveratrol; adipocyte; polychlorinated biphenyl; diabetes; Nrf2

1. Introduction

Polychlorinated biphenyls (PCBs) are persistent organic pollutants that are highly lipophilic and tend to bio-accumulate in the environment. Although industrial use of these compounds was banned in the U.S. in the 1970's, recent studies have estimated that the average American is exposed to approximately 33 ng of PCBs per day through the diet [1]. Several epidemiological studies suggest that exposure to low concentrations of PCBs may promote type 2 diabetes (T2D) in humans [2, 3]. Notably, recent results from the Anniston Community Health Survey demonstrated significant associations between elevated PCB levels and diabetes risk [4]. Largely resulting from accumulating evidence linking PCB exposures to diabetes, the National Institute of Environmental Health Studies (NIEHS), Division of the National Toxicology Program (NTP) hosted a workshop to review approximately seventy-five different epidemiology studies linking persistent organic pollutants (POPs), including coplanar PCBs, to T2D outcomes. A publication from the workshop concluded that there is evidence for a positive association between POP exposures and the development of T2D [5]. The summary of the workshop also called for additional studies to define mechanisms linking PCBs and other POPs to increased risk for diabetes.

We recently demonstrated that coplanar PCBs that are ligands of the aryl hydrocarbon receptor (AhR) impair glucose homeostasis in C57BL/6 mice [6]. These effects were associated with inflammation in adipose tissue, a site for pronounced PCB accumulation [6]. Similarly, recent studies demonstrated that 2,3,7,8-tetrachloro-dibenzo-*p*-dioxin (TCDD), an AhR ligand, promoted low grade inflammation in adipocytes in vitro and in vivo [7]. Generation of reactive oxygen species (ROS) by AhR ligands such as TCDD or PCBs in adipocytes may contribute to low grade inflammation and the development of insulin resistance [8].

The plant polyphenol, resveratrol (RSV), exerts several protective effects in adipocytes. In 3T3-L1 adipocytes, RSV inhibited stimulation of inflammatory adipokines [9-15]. Reductions in oxidative stress by RSV are associated with activation of nuclear factor erythoid 2-related factor 2 (Nrf2) [16-18], a component of the anti-oxidant pathway. RSV had been demonstrated to protect against insulin resistance in cultured adipocytes [19]. Moreover, administration of RSV improves glucose tolerance and reduces insulin resistance in mice with diet-induced obesity [20-22], in genetically obese rodents [23-25] and in humans with T2D [26]. Notably, RSV interacts with the AhR, resulting in translocation of the receptor to the nucleus; however this interaction does not appear to result in transactivation [27, 28]. Accordingly, RSV attenuates toxic effects of AhR ligands in vitro and in vivo [27, 29-32]. However, it is unclear if protective effects of RSV extend to PCB ligands of AhR, and whether this protection includes restoration of measures of insulin sensitivity in adipocytes, a primary site for PCB-induced activation of inflammatory cytokines that are linked to the development of insulin resistance [6, 33].

In this study, we tested the hypothesis that RSV protects against in vitro and in vivo effects of a coplanar PCB (PCB-77) to induce measures of insulin resistance. We selected coplanar PCB-77 for these studies based on its high toxicity and abundance within the food chain [34, 35, 36]. Since PCBs accumulate markedly in adipose tissue and have been demonstrated to promote inflammatory cytokines linked to insulin resistance [6, 33], we focused on adipocytes as the cell target of PCBs and/or RSV to regulate glucose homeostasis. As a mechanism for effects of PCB and/or RSV, we quantified oxidative stress and induction of the Nrf2 anti-oxidant signaling pathway. Our results suggest that RSV may provide therapeutic benefit against PCB-induced dysregulation of glucose homeostasis and the development of diabetes.

2. Methods

2.1 Materials

3,3',4,4'-tetrachlorobiphenyl (PCB-77) was purchased from AccuStandard Inc. (New Haven, CT). 2-deoxy-D-glucose (2DG), bovine insulin (0.1 μM for adipocyte differentiation), dexamethasone (1 μM), and isobutylmethyl xanthine (0.5 mM, IBMX) were obtained from Sigma Aldrich (St. Louis, MO). The resVida® (>99% pure transresveratrol) was provided by DSM Nutrition Products, Inc (Heerlen, NL).

2.2 Quantification of PCB-77, RSV, and metabolites in serum and tissues

PCB-77, hydroxyPCB-77 and RSV were measured using a Shimadzu UFLC coupled with an AB Sciex 4000-Qtrap hybrid linear ion trap triple quadrupole mass spectrometer in multiple reaction monitoring (MRM) mode. d6-PCB-77 was used as internal standard for PCB-77 and hydroxyPCB-77 measurements. D4-RSV was used as an internal standard for resveratrol and its metabolite measurements. The mass spectrometer was operated in the positive APCI mode for PCB-77 measurements and in negative ESI mode for hydroxyPCB-77 and RSV measurements with optimal ion source settings determined by synthetic standards. PCB-77 was analyzed using Kinetex 2.6 u C18, 100 A, 100 × 2.10 mm (Phenomenex) column. The mobile phase consisted of water as solvent A and acetonitrile as solvent B. For the analysis of PCBs the separation was achieved using a gradient of 20 % B to 60 % B for 1 min, 60% B to 100% B in the next 7 min, and maintained at 100% B for the last 2 min with a flow rate of 0.25 ml/min. MRM transitions monitored were as follows: 291.9/ 222.1 and 291.9/220 for PCB-77; and 297.9/228.1 and 297.9/226.2 for d6-PCB-77. In the MRM ion transition the precursor ion represents the M^+ and the product ion represents either $[M\text{-}Cl]^+$ or $[M\text{-}2Cl]^+$.

HydroxyPCB-77 was analyzed using Luna 3 u C18 (2), 100 A, 250 × 2.00 mm (Phenomenex) column with a flow rate of 0.25 mL/min. The mobile phase consisted of 75/25 of methanol/ water with formic acid (0.5%) and 5 mM ammonium formate (0.1%) as solvent A and 99/1of methanol/ water with formic acid (0.5%) and 5 mM ammonium formate (0.1%) as solvent B. HydroxyPCB-77 was eluted using a gradient of 10 % B to 100 % B in 4 min and maintained at 100% B for the next 11 min. MRM transitions monitored were as follows: 352.8/306.9 for hydroxyPCB-77 and 368.8/322.9 for dihydroxyPCB-77.

Precursor ion of the ion transition is a formic acid adduct: [M+FA-H]-and product ion is [M-H]-.

2.3 Cell culture

3T3-L1 mouse preadipocytes purchased from Zen-Bio (Research Triangle Park, NC) were cultured in standard Dulbecco's modified Eagle's medium (DMEM; Invitrogen, Carlsbad, CA) enriched with 10% fetal bovine serum (FBS; Gemini Bio-Products, Woodland, CA) and 1% penicillin/streptomycin in 6-well culture dishes. Cells (passage number 5 or lower) were grown to 100% confluence at 37°C in a humidified 5% CO2 atmosphere. Differentiation to mature adipocytes was induced as previously described [6]. Assays (n = 2/group) were performed in triplicate.

To examine the effects of PCBs, we incubated differentiated adipocytes (day 8) with vehicle [0.03% dimethyl sulfoxide (DMSO)] or PCB-77 (3.4 μM [6, 33]) for 24 hours in the absence or presence of RSV (0.1 μM, 1 μM, or 10 μM). RSV was added to culture media 30 minutes prior to the addition of vehicle or PCB-77. Cells were harvested for glucose uptake and oxidative stress assays in addition to mRNA quantification of gene expression.

2.4 Measurement of insulin-stimulated uptake of 2DG

To measure uptake of 2DG, differentiated 3T3-L1 adipocytes were incubated with appropriate treatments in serum-free media for 6 hours. Cells were washed three times and then incubated with insulin (1 μM) in glucose-free Krebs buffer (pH 7.4) containing 2% bovine serum albumin for 20 minutes at 37°C. 2DG (1 mM) was added to each well and incubated at 37°C for 20 minutes. Cells were washed three times with buffer, and 10 mM Tris-HCl was added to each well. Following sonication, cell lysates were collected and 2DG uptake was quantified per the manufacturer's instructions (2-Deoxyglucose Uptake Measurement kit, Cosmo Bio Co. Ltd., Tokyo, Japan). 2DG uptake was normalized to cellular protein.

2.5 Measurement of oxidative stress

To measure oxidative stress, differentiated 3T3-L1 adipocytes were incubated with appropriate treatments for 24 hours. Cellular oxidation was determined by 2',7'-dichlorofluorescein (DCF) fluorescence via the Oxiselect™ Intracellular ROS Assay kit (Cell Biolabs, Inc., San Diego, CA). Briefly, this method is based on the conversion of 2',7'-dichlorofluorescin into fluorescent DCF through oxidation by reactive oxygen species, including super oxide radicals and peroxides. Following appropriate treatments, cells were incubated with 100 μM 2',7'-dichlorofluorescin diacetate for 30 minutes. A multi-well fluorescent plate reader (Molecular Devices, CA) was utilized for measuring relative oxidative stress; excitation and emission wavelengths were 480 and 530 nm, respectively.

2.6 Animals and experimental diets

All experimental procedures met the approval of the Animal Care and Use Committee of the University of Kentucky. Two month old, male, C57BL/6 mice (The Jackson Laboratory, Bar Harbor, ME) were housed in a pathogen-free environment and given ad libutum access to water and standard mouse diet in the absence or presence of 0.1% resVida® (#5SSG, 14.6%

kcal as fat, TestDiet, Richmond, IN). Mice were pre-fed diets for 1 week prior to administration of vehicle (tocopherol stripped safflower oil, Dyets Inc., 10 μL/g of body weight) or PCB-77 (49.6 mg/kg)(n=10 mice/group), given in two divided doses during weeks 1 and 2. Body weights were recorded bi-weekly. Glucose and insulin tolerance tests were performed within 48 hours after the second dose as described below. At study endpoint, mice were fasted for 4 hours and anesthetized with ketamine/xylazine (100/10 mg/kg intraperitoneal (ip) injection). Following ketamine injection, a sub-set of mice in each group were injected (i.p.) with 10 U/kg body weight human insulin (Novolin) to stimulate insulin signaling pathways, using methods as described previously [37].

2.7 Glucose tolerance test (GTT) and insulin tolerance test (ITT)

For glucose (GTT) and insulin tolerance tests (ITT), sub-sets of mice in each group were examined within 48 hours after the second dose. Mice were fasted for 4 or 6 hours for ITT or GTT, respectively, and fasted blood glucose was measured by tail vein using a hand held glucometer (Freedom Freestyle Lite, Abbott Laboratories, Abbott Park, IL). Mice were injected (i.p.) with D-glucose (Sigma, 20% in saline, 10 μL/g of body weight) for GTT and blood glucose was measured at 15, 30, 60, 90, and 120 minutes later. For ITT, mice were injected (i.p.) with human insulin (Novolin, 0.0125 μM in saline/g of body weight), and plasma glucose was measured at 30, 60, 90, and 120 minutes later. Total area under the curve (AUC; arbitrary units) was calculated as previously described [6].

2.8 Quantification of adipose tissue Akt and P-Akt

For *in vivo* experiments, epididymal adipose tissue was homogenized and centrifuged, and supernatants were stored in 1X Cell Lysis Buffer (Cell Signaling, Danvers, MA). Akt and p-Akt concentrations were quantified as per the manufacturer's instructions using a commercial ELISA (Cell Signaling, Beverly, MA), and normalized to adipose tissue protein. For *in vitro* experiments, the identical method was used on cell lysate extracts.

2.9 RNA isolation and gene expression analysis using real-time polymerase chain reaction (PCR)

Total RNA was extracted from epididymal adipose tissue using the SV Total RNA Isolation System kit (Promega Corporation, Madison, WI), per the manufacturer's instructions. RNA from 3T3-L1 cells was extracted in Trizol. RNA concentrations were determined using a NanoDrop 2000 spectrophotometer and associated software (Thermo Scientific, Logan, UT). cDNA was synthesized from 0.4 μg total RNA with qScript cDNA SuperMix (Quanta Biosciences, Gaithersburg, MD) in the following reaction: 25°C for 5 minutes, 42°C for 30 minutes, and 85°C for 5 minutes. The cDNA was diluted 1:50 to achieve a concentration of 0.4 ng/μL. The diluted cDNA was amplified with an iCycler (Bio-Rad, Hercules, CA) and the Perfecta SYBR Green Fastmix for iQ (Quanta Biosciences, Gaithersburg, MD). Components of the PCR reaction were as follows: Perfecta SYBR Green FastMix (10 μL), forward and reverse primers (0.125 μL), nuclease free water (4.75 μL), and diluted cDNA (5 μL for 2 ng of cDNA/reaction). Using the difference from GAPDH (glyceraldehydes 3-phosphate dehydrogenase) rRNA (reference gene) and the comparative Ct method, the relative quantification of gene expression in each sample was calculated. Primers (Eurofins

MWG Operon, Huntsville, AL) were designed using the primer design program available from PubMed.gov (sequences presented in Table 1). The PCR reaction was as follows: 94°C for 5 minutes, 40 cycles at 94°C for 15 seconds, 58°C or 64°C (based on tested primer efficiency) for 40 seconds, 72°C for 10 minutes, and 100 cycles from 95°C to 45.5°C for 10 seconds.

2.10 Statistical analysis

Data are represented as mean ± standard error of the mean (SEM). Data was log transformed prior to statistical analysis. A one-way or two-way analysis of variance (ANOVA; SigmaPlot, version 12.0; Systat Software Inc., Chicago, IL) were used as appropriate to determine statistical significance, which was defined as $p < 0.05$. Glucose and insulin tolerance tests were analyzed using repeated measure, two-way ANOVA. Holm-Sidak method was used for post-hoc analyses, except in Figures 1D, 1E, and 4B which used Dunnett's method and basal and non-insulin stimulated groups as controls for comparison, respectively.

3. Results

3.1 RSV promotes Nrf2 signaling, suppresses oxidative stress, and restores insulin-stimulated glucose uptake in PCB-77 treated adipocytes

RSV has been demonstrated to promote the anti-oxidant Nrf2 signaling pathway and reduce oxidative stress in a variety of cell types [16-18]. We quantified effects of PCB-77 on Nrf2 and one of its downstream signaling targets, NQO1, and oxidative stress in the absence or presence of increasing concentrations of RSV in 3T3-L1 adipocytes. In the absence of RSV, PCB-77 had no significant effect on mRNA abundance of Nrf2 or NQO1 in 3T3-L1 adipocytes (Fig. 1A,B, respectively). However, in the presence of PCB-77, RSV significantly increased mRNA abundance of Nrf2 and NQO1 in a concentration-dependent manner (Fig. 1A,B; $P<0.05$). PCB-77 significantly increased fluorescence of DCF as a measure of oxidative stress, and this effect was abolished by RSV (1 μM; Fig. 1C, $P<0.05$).

To determine if PCB-77-induced oxidative stress influenced glucose homeostasis in 3T3-L1 adipocytes, and whether RSV could restore adipocyte function, we quantified the ratio of p-Akt to Akt as an index of insulin signaling, and 2DG uptake. The ratio of p-Akt to Akt was significantly increased by insulin and modestly increased further by RSV in insulin-stimulated cells (Fig. 1D; $P<0.05$). PCB-77 abolished insulin-stimulated pAkt, and this effect was reversed by RSV. In the presence of insulin, 2DG uptake increased 4-fold in 3T3-L1 adipocytes (DMSO *versus* basal; Fig. 1E, $P<0.05$). However, PCB-77 totally abolished 2DG uptake in insulin-stimulated adipocytes (Fig. 1E). Effects of PCB-77 to impair glucose uptake by adipocytes were reversed in a concentration-dependent manner by RSV (Fig. 1E, $P<0.05$).

3.2 RSV has no effect on tissue levels of PCB-77 or PCB-77 metabolites

RSV has been demonstrated to have AhR antagonist properties [27, 28], which could influence metabolism of PCBs by cytochrome P-450 1A1 (CYP1A1). We quantified mRNA abundance of CYP1A1 as an index of AhR activation in adipose tissue of mice administered

PCB-77 in the absence or presence of RSV. PCB-77 resulted in a significant increase in CYP1A1 mRNA abundance in adipose tissue of mice administered vehicle (VEH) or RSV (Fig. 2; $P<0.05$). We then quantified levels of PCB-77 and its major metabolites (hydroxyPCB-77, dihydroxyPCB-77) in serum, liver or adipose tissue from mice in each treatment group. Similarly, we quantified levels of the parent compound, trans-RSV, and 2 metabolites (RSV-3-O-glucuoride, trans-RSV-3-O-sulfate). As demonstrated previously [6], adipose tissue concentrations of PCB-77 were markedly higher than liver or serum (Table 2). Moreover, the ratio of PCB-77 to its quantified metabolites was greater in adipose tissue (5:1) than liver (0.02:1). Significantly higher concentrations of RSV metabolites were detected in serum, liver and adipose tissue than the parent molecule, RSV. Additionally, serum levels of the RSV metabolite, resveratrol-3-O-glucuronide, were significantly increased in mice administered PCB-77 compared to mice administered RSV alone. However, there was no significant effect of RSV on levels of PCB-77 or its metabolites.

3.3 RSV improves glucose tolerance and insulin signaling in adipose tissue of mice administered PCB-77

There was no significant effect of PCB-77 or RSV on body weight (data not shown). As reported previously [6], PCB-77 significantly impaired glucose and insulin tolerance (Fig. 3A,B, respectively), as indicated by a significant increase in the area under the curve (AUC) for blood glucose levels following administration of glucose (GTT) or insulin (ITT) (Fig. 3C,D, respectively). While RSV had no effect on either glucose or insulin tolerance in mice administered vehicle, RSV totally abolished effects of PCB-77 to impair glucose and insulin tolerance. Based on findings from 3T3-L1 adipocytes demonstrating that RSV stimulated the Nrf2 signaling cascade (Fig. 1A), we quantified mRNA abundance of Nrf2 and NQO1 in epididymal adipose tissue from insulin-stimulated mice. There was a modest, but insignificant effect of RSV to increase Nrf2 mRNA abundance in adipose tissue (Fig. 4A). However, in mice administered PCB-77, RSV resulted in a significant increase in mRNA abundance of NQO1 (Fig. 4B, $P<0.05$). We quantified levels of phosphorylated Akt (pAkt, normalized to total Akt) as an index of the insulin signaling pathway in adipose tissue of mice administered insulin. Administration of insulin significantly increased pAkt expression in adipose tissue, which was totally abolished by PCB-77 (Fig. 4C, $P<0.05$). While RSV had no effect in the absence of PCB-77, it totally restored insulin-stimulated levels of pAkt in adipose tissue (Fig. 4C, $P<0.05$).

4. Discussion

Results from this study demonstrate that supplementation with RSV in the diet totally prevents PCB-77 induced impairment of glucose and insulin tolerance in mice. Notably, PCB-77 resulted in pronounced suppression of insulin-stimulated levels of pAkt in adipose tissue, and this effect was abolished by RSV. In cultured adipocytes, PCB-77 increased oxidative stress and reduced insulin-stimulated ratios of p-Akt to Akt and glucose uptake, and these effects were attenuated in a concentration-dependent manner by RSV. Mechanisms of RSV to protect against PCB-induced oxidative stress and impairment of glucose uptake in 3T3-L1 adipocytes may involve activation of the anti-oxidant Nrf2 signaling pathway, as RSV stimulated Nrf2 and/or NQO1 expression in cultured adipocytes

and elevated NQO1 expression in adipose tissue of mice. In contrast, RSV did not alter systemic or tissue distribution of PCB-77 and/or its major metabolites, or levels of CYP1A1 in adipose tissue, suggesting that regulation of PCB metabolism did not contribute to effectiveness of RSV. In contrast, our results suggest that PCB-77 influenced serum levels of the RSV-3-O-glucuronide metabolite, as mice administered PCB-77 had significantly increased serum levels of this metabolite. It is conceivable that RSV metabolites contributed to the anti-diabetogenic effects of the compound in mice exposed to PCB-77. These results suggest that RSV can attenuate PCB-77-induced insulin resistance in adipose tissue potentially by stimulating the NRF2 pathway and preventing oxidative damage. RSV may provide an effective therapy to protect against PCB-induced dysregulation of glucose homeostasis.

Increasing evidence suggests that exposures to environmental pollutants, including PCBs, may be a contributing factor for an increased risk of T2D development. Similar to recent findings [6], in the present study administration of PCB-77 to C57BL/6 mice resulted in impaired glucose and insulin tolerance. Results from this study extend previous findings by demonstrating that PCB-77 administration totally abolished levels of phosphorylated Akt in adipose tissue as an index of insulin signaling. We recently reported that serum levels of PCB-77 in experimental mice are lower than total serum PCB levels in populations with known accidental exposures [6]. In the present study, mice administered PCB-77 had serum levels of approximately 0.07 ± 0.01 μM, consistent with total PCB levels reported in subjects from the highest quintile of the Anniston Community Health Survey Population that exhibit an increased odds ratio for T2D [4]. Moreover, as reported previously [6, 38], PCB-77 accumulated markedly in adipose tissue compared to serum or liver. An interesting finding of the present study was the higher ratio of parent PCB-77 compound to its metabolites in adipose tissue, as compared to liver. These results suggest that in comparison to liver where PCBs are predominately metabolized through CYP1A1 activation, sequestration of the parent PCB-77 molecule in adipose lipids may hinder effective metabolism of the toxin. However, upon release of sequestered PCBs from adipose tissue during lipolysis, adipocytes may experience more pronounced effects of the toxin at adipocyte AhR.

In the present study, serum RSV concentrations (0.6 nM) in 4 hour fasted mice were lower than concentrations (1 μM) that effectively abolished PCB-77 induced oxidative stress and impaired glucose uptake by 3T3-L1 adipocytes. Previous investigators demonstrated that fasted (4 hrs) C57BL/6 mice administered 100 mg/kg of RSV via oral gavage had appreciable amounts of the RSV-3-O-glucuronide metabolite [39]. These results suggest that protective effects of RSV observed during fasting of mice in this study may have resulted from RSV metabolites. In humans and rats less than 5% of the oral dose has been reported as the parent molecule RSV in blood [40-44]. The most abundant RSV metabolites in humans, rats, and mice are trans-resveratrol-3-O-glucuronide and trans-resveratrol-3-sulfate [45]. There are conflicting reports in reference to the active source of RSV bioactivity (e.g., parent compound, sulfate or glucuronide metabolites) [40, 41, 46]. Importantly, tissue levels of PCB-77 and metabolites were not influenced by co-administration of RSV to mice, suggesting that protective effects of RSV against PCB-induced impairment of glucose homeostasis did not result from changes in distribution or metabolism of PCB-77.

In the present study we demonstrated that supplementation with RSV effectively protected against the diabetogenic effects of PCB-77 in vitro and in vivo. A recent clinical study of T2D patients treated with oral RSV supplements for three months reported significant improvements in nearly all biomarkers associated with the disease [26]. However, other groups have not been able to show improvements in insulin sensitivity or glucose regulation with RSV [47, 48]. The dietary dose of RSV used in this study (approx. 160 mg/kg/day) equates to a human equivalent dose of just under 800 mg/day for a 60 kg individual [49]. This dose of RSV would not be achievable in humans without the aid of supplementation. A potential RSV treatment therapy in PCB exposed populations should be regarded cautiously, since the drug interaction potential of the high doses of RSV typically utilized in clinical trials remains poorly understood [50]. Interestingly, plant food sources that are high in RSV also tend to be conversely low in PCBs, as total PCB concentrations in food tend to be higher in meats and fish than other sources [1]. This would suggest that a diet that enhances consumption of vegetables and limits PCB containing foods (e.g., meat) would simultaneously confer antioxidant protection and lower the total body burden of these environmental contaminants.

Another interesting finding from this study was that RSV had little effect on any measured parameter in the absence of PCB-77 administration. This finding is consistent with recent studies that demonstrate that RSV had no effect in lean individuals [47], or that RSV improved adipose tissue glucose homeostasis only under insulin resistant conditions [19]. These results suggest that RSV would not adversely influence glucose homeostasis in the absence of an insult, in this case, exposure to an environmental toxin. Indeed, protective pathways (e.g., NQO1) targeted by RSV are typically quiescent and become activated in response to an external stimuli (e.g., PCB-77).

Mechanisms for protective effects of RSV in the present study include reductions in oxidative stress associated with stimulation of the anti-oxidant Nrf2 signaling pathway. Emerging research has focused on the interaction of the Nrf2 system with insulin action, demonstrating that insulin and its effector Akt/PKB modulate the function of Nrf2. In *Caenorhabditis elegans*, it was demonstrated that Nrf2 can be directly phosphorylated by Akt, which represses its nuclear translocation [51]. Several studies in mammals have shown that insulin signaling is required for Nrf2 activation [52, 53]. Nrf2 function is defective in aged mice [54] and aging is typically accompanied by insulin resistance. It is unclear if impaired insulin signaling blunts Nrf2 function or vice versa. Several studies have demonstrated that RSV stimulates Nrf2 expression in various cell types [16-18]. As described above, RSV stimulated Nrf2 and NQO1 gene expression only in adipocytes incubated with PCB-77, suggesting that stimulation of the anti-oxidant system by RSV requires induction of oxidative stress by a damaging stimulus. These results are consistent with in vivo data from the present study demonstrating that RSV favorably influenced a measure of insulin signaling and NQO1 gene expression in adipose tissue only when mice were exposed to PCB-77.

In conclusion, results from this study indicate that RSV reduces PCB-77 induced oxidative stress in adipose tissue while simultaneously enhancing Nrf2 signaling. RSV-mediated stimulation of Nrf2 signaling may have contributed to protection from PCB-77-induced

impairment of glucose and insulin tolerance. These results suggest that supplementation with resveratrol may be a potential therapy for populations with known PCB exposures to lower the risk of developing diabetes.

Acknowledgments

Grants, Sponsors & Funding: This work was supported by grants from the National Institute of Environmental Health Sciences (P42 ES 007380, LAC), the National Institute of Diabetes and Digestive and Kidney Diseases (T32 3048107792, NAB, LAC), and the National Institute of General Medical Sciences (P20GM103527, LAC). The authors thank DSM Nutritional Products for providing the resVida® for the study.

References

1. Schecter A, Colacino J, Haffner D, Patel K, Opel M, Papke O, et al. Perfluorinated compounds, polychlorinated biphenyls, and organochlorine pesticide contamination in composite food samples from Dallas, Texas, USA. Environ Health Perspect. 2010; 118:796–802. [PubMed: 20146964]
2. Lee DH, Steffes MW, Sjodin A, Jones RS, Needham LL, Jacobs DR Jr. Low dose of some persistent organic pollutants predicts type 2 diabetes: a nested case-control study. Environ Health Perspect. 2010; 118:1235–42. [PubMed: 20444671]
3. Lee DH, Steffes MW, Sjodin A, Jones RS, Needham LL, Jacobs DR Jr. Low dose organochlorine pesticides and polychlorinated biphenyls predict obesity, dyslipidemia, and insulin resistance among people free of diabetes. PLoS One. 2011; 6:e15977. [PubMed: 21298090]
4. Silverstone AE, Rosenbaum PF, Weinstock RS, Bartell SM, Foushee HR, Shelton C, et al. Polychlorinated biphenyl (PCB) exposure and diabetes: results from the Anniston Community Health Survey. Environ Health Perspect. 2012; 120:727–32. [PubMed: 22334129]
5. Thayer KA, Heindel JJ, Bucher JR, Gallo MA. Role of environmental chemicals in diabetes and obesity: a National Toxicology Program workshop review. Environ Health Perspect. 2012; 120:779–89. [PubMed: 22296744]
6. Baker NA, Karounos M, English V, Fang J, Wei Y, Stromberg A, et al. Coplanar polychlorinated biphenyls impair glucose homeostasis in lean C57BL/6 mice and mitigate beneficial effects of weight loss on glucose homeostasis in obese mice. Environ Health Perspect. 2013; 121:105–10. [PubMed: 23099484]
7. Kim MJ, Pelloux V, Guyot E, Tordjman J, Bui LC, Chevallier A, et al. Inflammatory pathway genes belong to major targets of persistent organic pollutants in adipose cells. Environ Health Perspect. 2012; 120:508–14. [PubMed: 22262711]
8. Kern PA, Fishman RB, Song W, Brown AD, Fonseca V. The effect of 2,3,7,8-tetrachlorodibenzo-p-dioxin (TCDD) on oxidative enzymes in adipocytes and liver. Toxicology. 2002; 171:117–25. [PubMed: 11836018]
9. Ahn J, Lee H, Kim S, Ha T. Resveratrol inhibits TNF-alpha-induced changes of adipokines in 3T3-L1 adipocytes. Biochem Biophys Res Commun. 2007; 364:972–7. [PubMed: 17967414]
10. Zhu J, Yong W, Wu X, Yu Y, Lv J, Liu C, et al. Anti-inflammatory effect of resveratrol on TNF-alpha-induced MCP-1 expression in adipocytes. Biochem Biophys Res Commun. 2008; 369:471–7. [PubMed: 18291098]
11. Szkudelska K, Nogowski L, Szkudelski T. Resveratrol, a naturally occurring diphenolic compound, affects lipogenesis, lipolysis and the antilipolytic action of insulin in isolated rat adipocytes. J Steroid Biochem Mol Biol. 2009; 113:17–24. [PubMed: 19041941]
12. Yen GC, Chen YC, Chang WT, Hsu CL. Effects of polyphenolic compounds on tumor necrosis factor-alpha (TNF-alpha)-induced changes of adipokines and oxidative stress in 3T3-L1 adipocytes. J Agric Food Chem. 2011; 59:546–51. [PubMed: 21186817]
13. Olholm J, Paulsen SK, Cullberg KB, Richelsen B, Pedersen SB. Anti-inflammatory effect of resveratrol on adipokine expression and secretion in human adipose tissue explants. Int J Obes (Lond). 2010; 34:1546–53. [PubMed: 20531350]

14. Kang L, Heng W, Yuan A, Baolin L, Fang H. Resveratrol modulates adipokine expression and improves insulin sensitivity in adipocytes: Relative to inhibition of inflammatory responses. Biochimie. 2010; 92:789–96. [PubMed: 20188786]
15. Rosenow A, Noben JP, Jocken J, Kallendrusch S, Fischer-Posovszky P, Mariman EC, et al. Resveratrol-induced changes of the human adipocyte secretion profile. J Proteome Res. 2012; 11:4733–43. [PubMed: 22905912]
16. He X, Wang L, Szklarz G, Bi Y, Ma Q. Resveratrol inhibits paraquat-induced oxidative stress and fibrogenic response by activating the nuclear factor erythroid 2-related factor 2 pathway. J Pharmacol Exp Ther. 2012; 342:81–90. [PubMed: 22493042]
17. Palsamy P, Subramanian S. Resveratrol protects diabetic kidney by attenuating hyperglycemia-mediated oxidative stress and renal inflammatory cytokines via Nrf2-Keap1 signaling. Biochim Biophys Acta. 2011; 1812:719–31. [PubMed: 21439372]
18. Cheng AS, Cheng YH, Chiou CH, Chang TL. Resveratrol upregulates Nrf2 expression to attenuate methylglyoxal-induced insulin resistance in Hep G2 cells. J Agric Food Chem. 2012; 60:9180–7. [PubMed: 22917016]
19. Kang W, Hong HJ, Guan J, Kim DG, Yang EJ, Koh G, et al. Resveratrol improves insulin signaling in a tissue-specific manner under insulin-resistant conditions only: in vitro and in vivo experiments in rodents. Metabolism. 2012; 61:424–33. [PubMed: 21945106]
20. Baur JA, Pearson KJ, Price NL, Jamieson HA, Lerin C, Kalra A, et al. Resveratrol improves health and survival of mice on a high-calorie diet. Nature. 2006; 444:337–42. [PubMed: 17086191]
21. Lagouge M, Argmann C, Gerhart-Hines Z, Meziane H, Lerin C, Daussin F, et al. Resveratrol improves mitochondrial function and protects against metabolic disease by activating SIRT1 and PGC-1alpha. Cell. 2006; 127:1109–22. [PubMed: 17112576]
22. Jeon BT, Jeong EA, Shin HJ, Lee Y, Lee DH, Kim HJ, et al. Resveratrol attenuates obesity-associated peripheral and central inflammation and improves memory deficit in mice fed a high-fat diet. Diabetes. 2012; 61:1444–54. [PubMed: 22362175]
23. Chen S, Li J, Zhang Z, Li W, Sun Y, Zhang Q, et al. Effects of resveratrol on the amelioration of insulin resistance in KKAy mice. Can J Physiol Pharmacol. 2012; 90:237–42. [PubMed: 22309033]
24. Rivera L, Moron R, Zarzuelo A, Galisteo M. Long-term resveratrol administration reduces metabolic disturbances and lowers blood pressure in obese Zucker rats. Biochem Pharmacol. 2009; 77:1053–63. [PubMed: 19100718]
25. Milne JC, Lambert PD, Schenk S, Carney DP, Smith JJ, Gagne DJ, et al. Small molecule activators of SIRT1 as therapeutics for the treatment of type 2 diabetes. Nature. 2007; 450:712–6. [PubMed: 18046409]
26. Bhatt JK, Thomas S, Nanjan MJ. Resveratrol supplementation improves glycemic control in type 2 diabetes mellitus. Nutr Res. 2012; 32:537–41. [PubMed: 22901562]
27. Casper RF, Quesne M, Rogers IM, Shirota T, Jolivet A, Milgrom E, et al. Resveratrol has antagonist activity on the aryl hydrocarbon receptor: implications for prevention of dioxin toxicity. Mol Pharmacol. 1999; 56:784–90. [PubMed: 10496962]
28. Beedanagari SR, Bebenek I, Bui P, Hankinson O. Resveratrol inhibits dioxin-induced expression of human CYP1A1 and CYP1B1 by inhibiting recruitment of the aryl hydrocarbon receptor complex and RNA polymerase II to the regulatory regions of the corresponding genes. Toxicol Sci. 2009; 110:61–7. [PubMed: 19376845]
29. Ishida T, Takeda T, Koga T, Yahata M, Ike A, Kuramoto C, et al. Attenuation of 2,3,7,8-tetrachlorodibenzo-p-dioxin toxicity by resveratrol: a comparative study with different routes of administration. Biol Pharm Bull. 2009; 32:876–81. [PubMed: 19420757]
30. Chen ZH, Hurh YJ, Na HK, Kim JH, Chun YJ, Kim DH, et al. Resveratrol inhibits TCDD-induced expression of CYP1A1 and CYP1B1 and catechol estrogen-mediated oxidative DNA damage in cultured human mammary epithelial cells. Carcinogenesis. 2004; 25:2005–13. [PubMed: 15142886]
31. Lu C, Bambang IF, Armstrong JS, Whiteman M. Resveratrol blocks high glucose-induced mitochondrial reactive oxygen species production in bovine aortic endothelial cells: role of phase 2 enzyme induction? Diabetes Obes Metab. 2008; 10:347–9. [PubMed: 18333893]

32. Singh NP, Singh US, Nagarkatti M, Nagarkatti PS. Resveratrol (3,5,4'-trihydroxystilbene) protects pregnant mother and fetus from the immunotoxic effects of 2,3,7,8-tetrachlorodibenzo-p-dioxin. Mol Nutr Food Res. 2011; 55:209–19. [PubMed: 20715097]
33. Arsenescu V, Arsenescu RI, King V, Swanson H, Cassis LA. Polychlorinated biphenyl-77 induces adipocyte differentiation and proinflammatory adipokines and promotes obesity and atherosclerosis. Environ Health Perspect. 2008; 116:761–8. [PubMed: 18560532]
34. McFarland VA, Clarke JU. Environmental occurrence, abundance, and potential toxicity of polychlorinated biphenyl congeners: considerations for a congener-specific analysis. Environ Health Perspect. 1989; 81:225–39. [PubMed: 2503374]
35. Hansen LG. Stepping backward to improve assessment of PCB congener toxicities. Environ Health Perspect. 1998; 106(Suppl 1):171–89. [PubMed: 9539012]
36. Fernandez-Gonzalez R, Yebra-Pimental I, Martinez-Carballo E, Requeiro J, Simal-Gandara J. Inputs of polychlorinated biphenyl residues in animal feeds. Food Chem. 2013; 140(1-2):296–304. [PubMed: 23578646]
37. Kienesberger PC, Lee D, Pulinilkunnil T, Brenner DS, Cai L, Magnes C, et al. Adipose triglyceride lipase deficiency causes tissue-specific changes in insulin signaling. J Biol Chem. 2009; 284:30218–29. [PubMed: 19723629]
38. Kodavanti PR, Ward TR, Derr-Yellin EC, Mundy WR, Casey AC, Bush B, et al. Congener-specific distribution of polychlorinated biphenyls in brain regions, blood, liver, and fat of adult rats following repeated exposure to Aroclor 1254. Toxicol Appl Pharmacol. 1998; 153:199–210. [PubMed: 9878591]
39. Johnson JJ, Nihal M, Siddiqui IA, Scarlett CO, Bailey HH, Mukhtar H, et al. Enhancing the bioavailability of resveratrol by combining it with piperine. Mol Nutr Food Res. 2011; 55:1169–76. [PubMed: 21714124]
40. Walle T, Hsieh F, DeLegge MH, Oatis JE Jr. Walle UK. High absorption but very low bioavailability of oral resveratrol in humans. Drug Metab Dispos. 2004; 32:1377–82. [PubMed: 15333514]
41. Boocock DJ, Patel KR, Faust GE, Normolle DP, Marczylo TH, Crowell JA, et al. Quantitation of trans-resveratrol and detection of its metabolites in human plasma and urine by high performance liquid chromatography. J Chromatogr B Analyt Technol Biomed Life Sci. 2007; 848:182–7.
42. Wenzel E, Soldo T, Erbersdobler H, Somoza V. Bioactivity and metabolism of trans-resveratrol orally administered to Wistar rats. Mol Nutr Food Res. 2005; 49:482–94. [PubMed: 15779067]
43. Marier JF, Vachon P, Gritsas A, Zhang J, Moreau JP, Ducharme MP. Metabolism and disposition of resveratrol in rats: extent of absorption, glucuronidation, and enterohepatic recirculation evidenced by a linked-rat model. J Pharmacol Exp Ther. 2002; 302:369–73. [PubMed: 12065739]
44. Abd El-Mohsen M, Bayele H, Kuhnle G, Gibson G, Debnam E, Kaila Srai S, et al. Distribution of [3H]trans-resveratrol in rat tissues following oral administration. Br J Nutr. 2006; 96:62–70. [PubMed: 16869992]
45. Yu C, Shin YG, Chow A, Li Y, Kosmeder JW, Lee YS, et al. Human, rat, and mouse metabolism of resveratrol. Pharm Res. 2002; 19:1907–14. [PubMed: 12523673]
46. Wang LX, Heredia A, Song H, Zhang Z, Yu B, Davis C, et al. Resveratrol glucuronides as the metabolites of resveratrol in humans: characterization, synthesis, and anti-HIV activity. J Pharm Sci. 2004; 93:2448–57. [PubMed: 15349955]
47. Yoshino J, Conte C, Fontana L, Mittendorfer B, Imai S, Schechtman KB, et al. Resveratrol supplementation does not improve metabolic function in nonobese women with normal glucose tolerance. Cell Metab. 2012; 16:658–64. [PubMed: 23102619]
48. Poulsen MM, Vestergaard PF, Clasen BF, Radko Y, Christensen LP, Stodkilde-Jorgensen H, et al. High-dose resveratrol supplementation in obese men: an investigator-initiated, randomized, placebo-controlled clinical trial of substrate metabolism, insulin sensitivity, and body composition. Diabetes. 2013; 62:1186–95. [PubMed: 23193181]
49. Reagan-Shaw S, Nihal M, Ahmad N. Dose translation from animal to human studies revisited. FASEB J. 2008; 22:659–61. [PubMed: 17942826]
50. Detampel P, Beck M, Krahenbuhl S, Huwyler J. Drug interaction potential of resveratrol. Drug Metab Rev. 2012; 44:253–65. [PubMed: 22788578]

51. Tullet JM, Hertweck M, An JH, Baker J, Hwang JY, Liu S, et al. Direct inhibition of the longevity-promoting factor SKN-1 by insulin-like signaling in C. elegans. Cell. 2008; 132:1025–1038. [PubMed: 18358814]

52. Chang CL, Au LC, Huang SW, Fai Kwok C, Ho LT, Juan CC. Insulin up-regulates heme oxygenase-1 expression in 3T3-L1 adipocytes via PI3-kinase- and PKC-dependent pathways and heme oxygenase-1-associated microRNA downregulation. Endocrinology. 2011; 152:384–393. [PubMed: 21147878]

53. Geraldes P, Yagi K, Ohshiro Y, He Z, Maeno Y, Yamamoto-Hiraoka J, et al. Selective regulation of heme oxygenase-1 expression and function by insulin through IRS1/phosphoinositide 3-kinase/Akt-2 pathway. J Biol Chem. 2008; 283:34327–34336. [PubMed: 18854316]

54. Morrison CD, Pistell PJ, Ingram DK, Johnson WD, Liu Y, Fernandez-Kim SO, et al. High fat diet increases hippocampal oxidative stress and cognitive impairment in aged mice: implications for decreased Nrf2 signaling. J Neurochem. 2010; 114:1581–1589. [PubMed: 20557430]

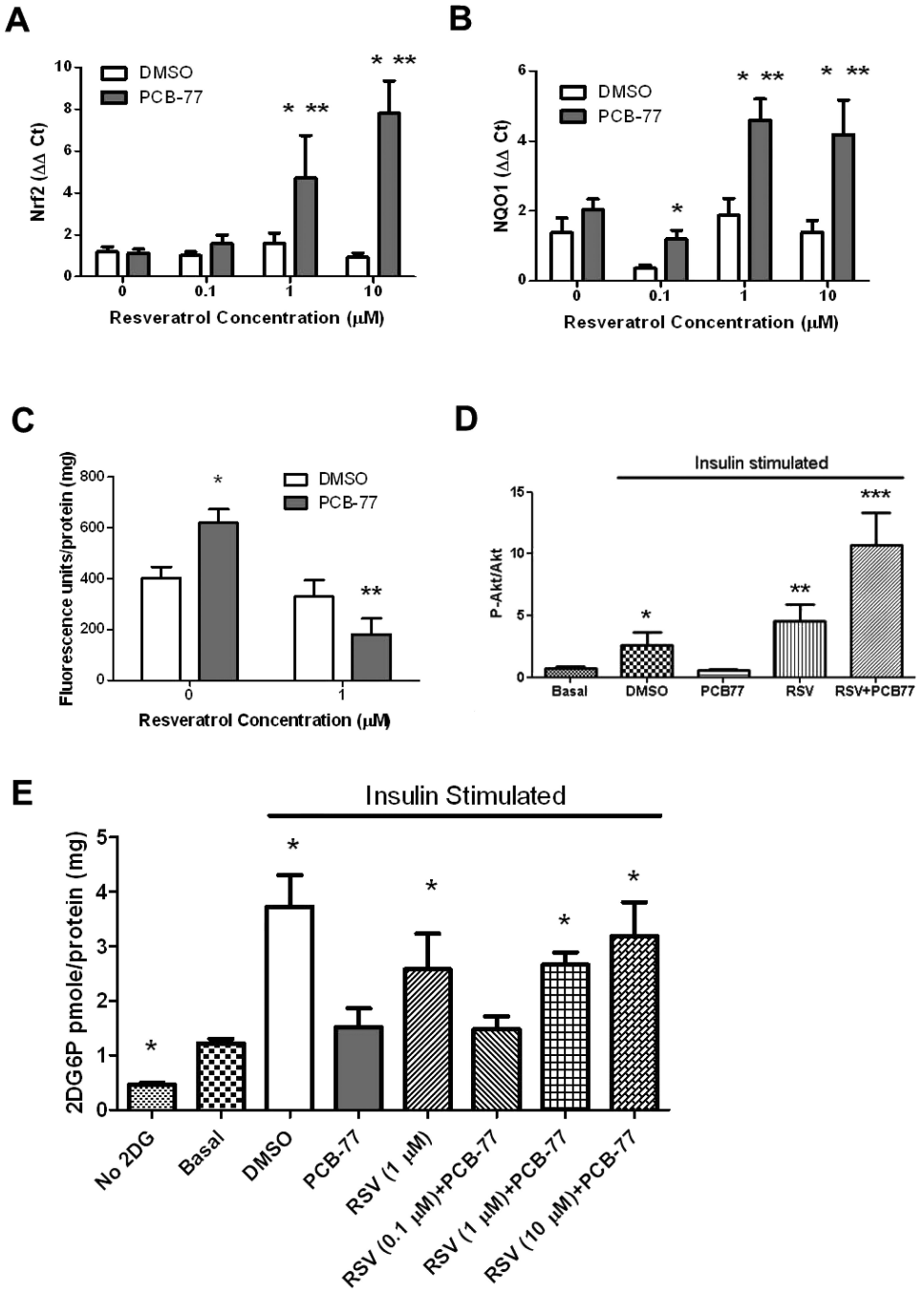

Figure 1.

Resveratrol protects 3T3-L1 adipocytes against PCB-77-induced oxidative stress and impaired glucose uptake. A, RSV results in a concentration-dependent increase in Nrf2 mRNA abundance in 3T3-L1 adipocytes incubated with PCB-77 (3.4 μM). B, RSV (1, 10 μM) promotes NQO1 mRNA abundance in 3T3-L1 adipocytes incubated with PCB-77. C, PCB-77 increases DCF fluorescence as an index of oxidative stress, which is abolished by RSV (1 μM). D, PCB-77 abolishes insulin-stimulated ratios of p-Akt to Akt in 3T3-L1 adipocytes, and RSV (1 μM) restores this ratio. E, PCB-77 abolishes insulin-stimulated 2DG

uptake in 3T3-L1 adipocytes, and RSV restores insulin-stimulated glucose uptake. Data are mean ± SEM from n = 2 experimental triplicates. *, P<0.05 compared to DMSO within RSV concentration or compared to basal in Figure 1D and 1E; **, P<0.05 compared to 0 within treatment in Figure 1A and 1B or P<0.01 in Figure 1D; ***, P<0.001 in Figure 1D.

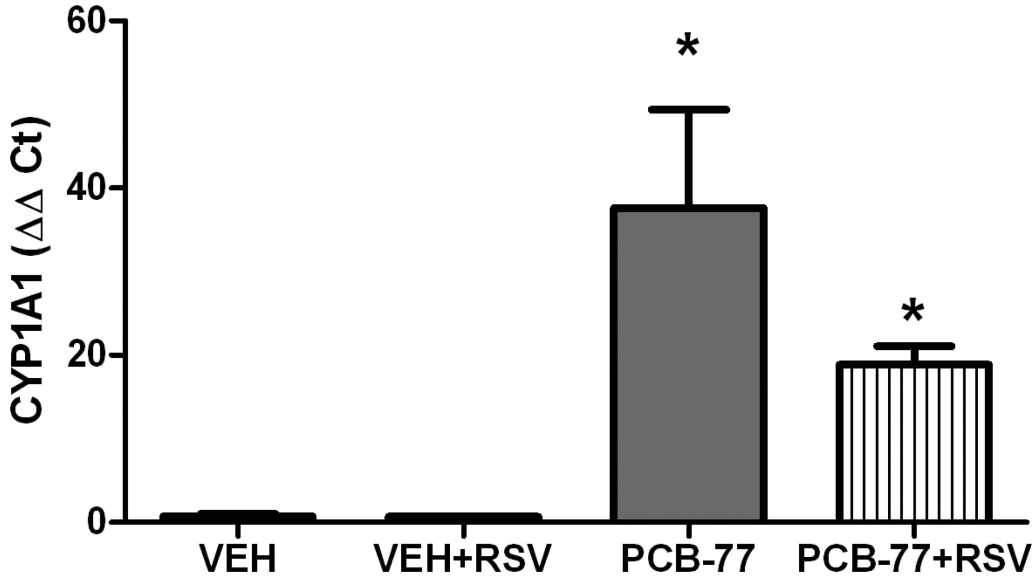

Figure 2.

PCB-77 increases CYP1A1 mRNA abundance in adipose tissue. Mice were administered vehicle (VEH) or PCB-77 (50 mg/kg) in 2 divided doses and fed standard mouse diet without and with RSV (0.1%). At 48 hours after the second PCB-77 dose, adipose tissue was harvested for quantification of gene expression. PCB-77 administration significantly increased CYP1A1 mRNA abundance in adipose tissue of mice in each diet group. Data are mean ± SEM from n = 5 mice/group. *, $P<0.05$ compared to VEH within diet group.

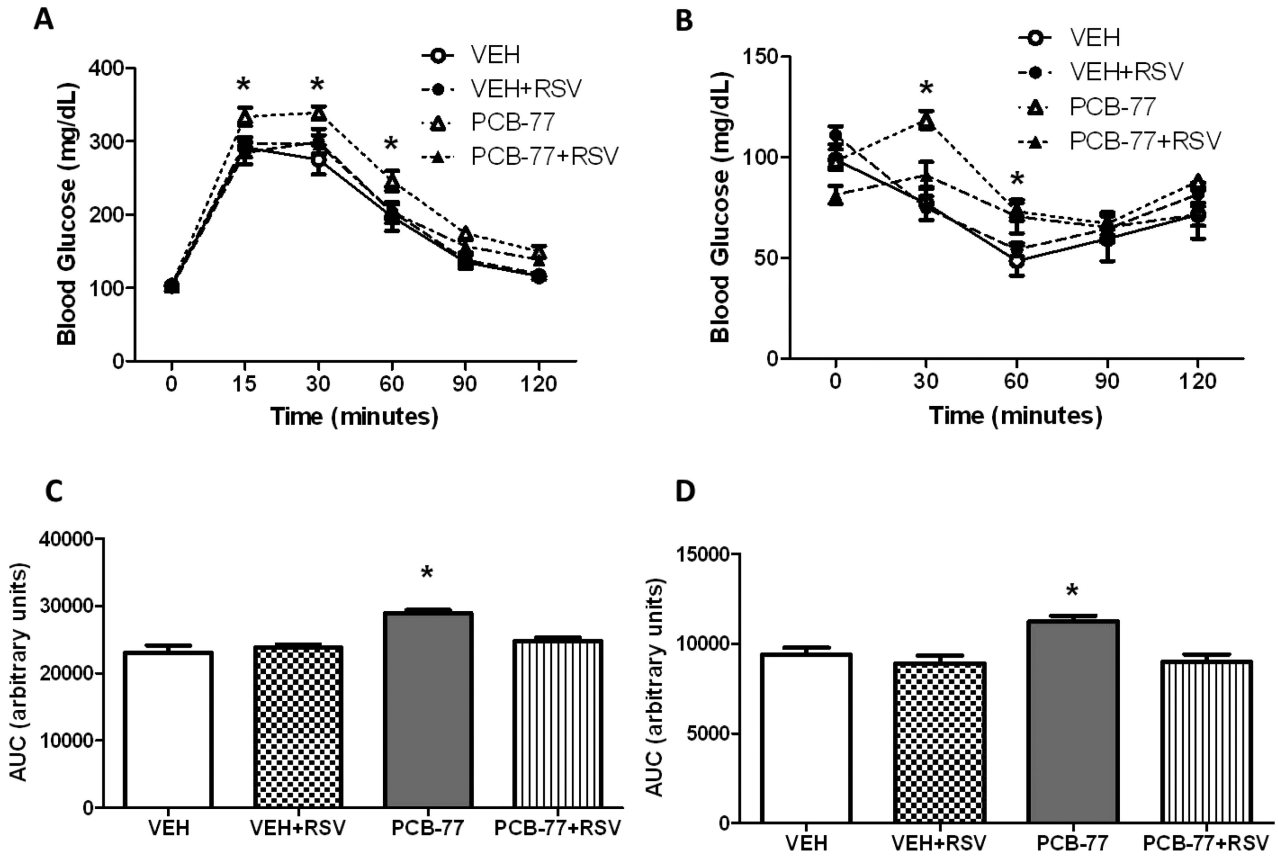

Figure 3.

RSV prevents PCB-77-induced impairment of glucose or insulin tolerance. Mice were administered vehicle (VEH) or PCB-77 (50 mg/kg) in 2 divided doses. Mice in each treatment group were fed either standard mouse diet or diet enriched with Resvida™ (RSV, 0.1%). A, Blood glucose levels after administration of glucose. B, Blood glucose levels after administration of insulin. C, Area under the curve (AUC) for data in A. D, AUC for data in B. Data are mean ± SEM from n = 5 mice/group. *, P<0.05 compared to PCB77+RSV (A,B) or compared to VEH (C,D).

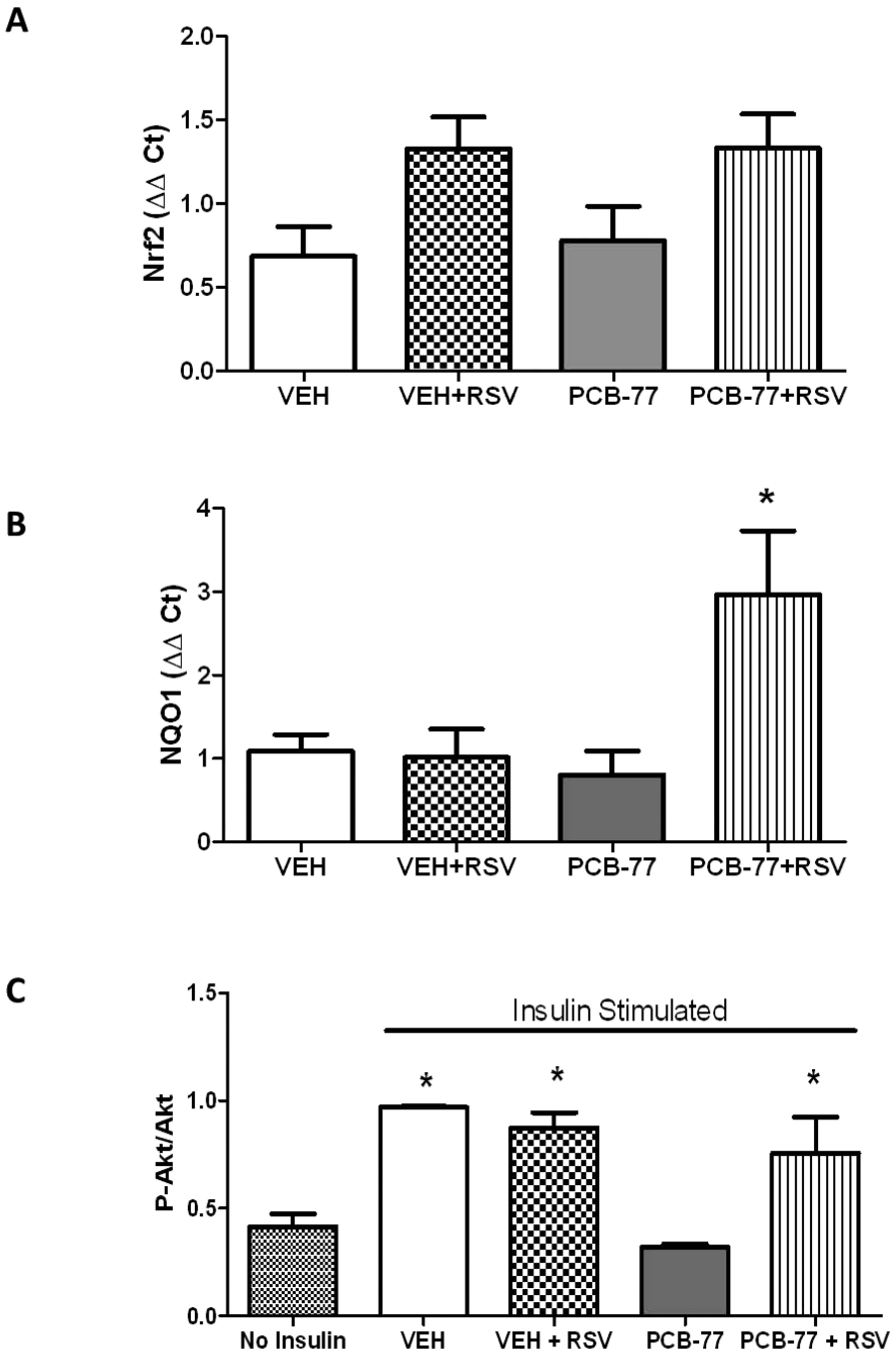

Figure 4.

RSV promotes the anti-oxidant NRF2 target, NQO1, and reverses PCB-77-induced impairment of insulin signaling in adipose tissue. Mice were administered vehicle (VEH) or PCB-77 (50 mg/kg) in 2 divided doses, and fed either standard mouse diet or a diet enriched with RSV (0.01%). A, Nrf2 mRNA abundance in adipose tissue from mice in each treatment group. B, NQO1 mRNA abundance in adipose tissue from mice in each treatment group. C, Levels of phosphorylated Akt (pAkt), normalized to total Akt, in adipose tissue from mice in each treatment group in the absence (no insulin) or presence of insulin. Data are mean ±

SEM from n = 5 mice/group. *, P<0.05 compared to VEH (A) or compared to no insulin (B).

Table 1

Primer sequences for real-time PCR.

Gene	Forward	Reverse
CYP1A1	AGTCAATCTGAGCAATGAGTTTGG	GGCATCCAGGGAAGAGTTAGG
GAPDH	GCCAAAAGGGTCATCATCTC	GGCCATCCACAGTCTTCT
NQO1	AGGATGGGAGGTACTCGAATC	TGCTAGAGATGACTCGGAAGG
Nrf2	CCATATTCCATTCCCTGTCG	TAAGTGGCCCAAGTCTTGCT

Abbreviations: CYP1A1, cytochrome P-450 1A1; GAPDH, glyceraldehyde 3-phosphate dehydrogenase; NQO1, NAD(P)H:quinone oxidoreductase 1; Nrf2, nuclear factor erythoid 2-related factor 2.

Table 2

Levels of PCB-77, RSV, and their metabolites in serum, liver, and retroperitoneal fat of mice.

PCB-77 (μM)				
Tissue type	VEH	VEH+RSV	PCB-77	PCB-77+RSV
Serum	N.D.	N.D.	0.07 ± 0.01	0.08 ± 0.01
Liver	N.D.	N.D.	4.78 ± 1.29	3.16 ± 0.98
RPF	N.D.	N.D.	29.90 ± 5.99	19.12 ± 3.87
HydroxyPCB-77 (μM)				
Tissue type	VEH	VEH+RSV	PCB-77	PCB-77+RSV
Serum	N.D.	N.D.	1.53 ± 0.17	1.73 ± 0.22
Liver	N.D.	N.D.	216.19 ± 134.87	75.22 ± 30.87
RPF	N.D.	N.D.	4.25 ± 0.79	3.14 ± 0.54
DihydroxyPCB-77 (μM)				
Tissue type	VEH	VEH+RSV	PCB-77	PCB-77+RSV
Serum	N.D.	N.D.	0.31 ± 0.04	0.45 ± 0.06
Liver	N.D.	N.D.	1.50 ± 0.93	2.39 ± 2.00
RPF	N.D.	N.D.	1.77 ± 0.49	1.21 ± 0.15
Resveratrol (nM)				
Tissue type	VEH	VEH+RSV	PCB-77	PCB-77+RSV
Serum	N.D.	0.60 ± 0.08	N.D.	0.75 ± 0.07
Liver	N.D.	0.08 ± 0.03	N.D.	0.06 ± 0.04
RPF	N.D.	0.57 ± 0.32	N.D.	2.87 ± 1.54
Resveratrol-3-O-glucuronide (nM)				
Tissue type	VEH	VEH+RSV	PCB-77	PCB-77+RSV
Serum	N.D.	43.40 + 14.71	N.D.	180.06 ± 39.26*
Liver	N.D.	13.15 ± 10.79	N.D.	7.24 ± 1.68
RPF	N.D.	1.11 ± 0.24	N.D.	1.97 ± 0.45
Resveratrol-3-O-sulfate (nM)				
Tissue type	VEH	VEH+RSV	PCB-77	PCB-77+RSV
Serum	N.D.	34.06 ± 8.91	N.D.	30.95 ± 4.09
Liver	N.D.	17.34 ± 8.59	N.D.	62.63 ± 37.46
RPF	N.D.	0.99 ± 0.28	N.D.	3.58 ± 1.48

Values are mean ± SEM from n ≥ 5/group.

VEH, vehicle; RSV, resveratrol; RPF, retroperitoneal fat.

*P<0.05 compared to VEH within diet group, as compared by Student's t-test.